Spatiotemporal PET reconstruction using total variation based priors

Maïtine Bergounioux[1], Evangelos Papoutsellis[1,2], Clovis Tauber[2], Simon Stute[3]

[1]Institut Denis Poisson, [2]Inserm UMR1253 iBrain
[3]Institut des sciences du vivant Frédéric Joliot, Paris

Journée Scientifique Cascimodot

June, 2018

Outline

- ☑ Motivation
- ☑ Dynamic PET
- ☑ Variational framework in PET
- ☑ TV based priors
- ☑ Numerical implementation
- ☑ Dynamic PET simulation

☑ Motivation

Motivation

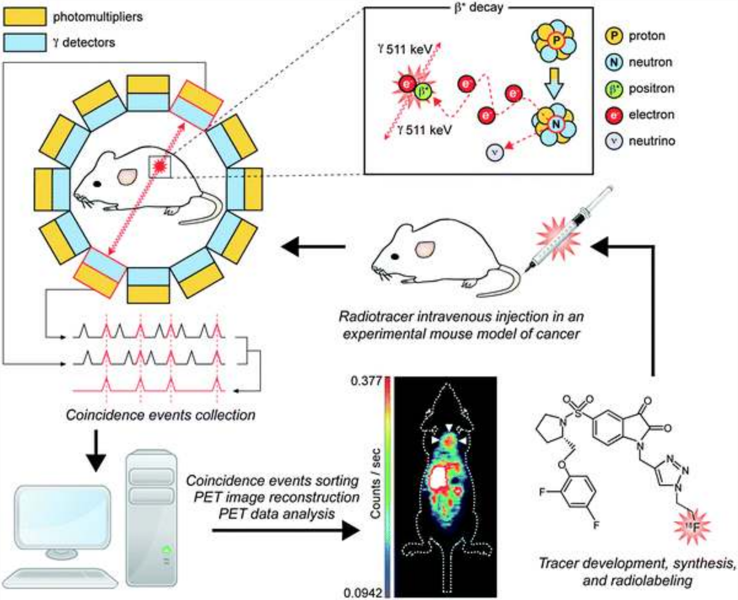
photomultipliers
γ detectors
β⁺ decay
γ 511 keV
γ 511 keV
proton
neutron
positron
electron
neutrino
Radiotracer intravenous injection in an experimental mouse model of cancer
Coincidence events collection
Coincidence events sorting
PET image reconstruction
PET data analysis
0.377
Counts / sec
0.0942
Tracer development, synthesis, and radiolabeling

☑ Dynamic PET

Dynamic PET

Measure changes in the biodistribution of radiopharmaceuticals within organs of interest over time.

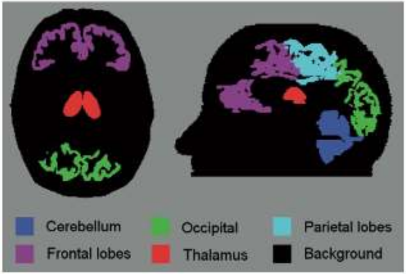

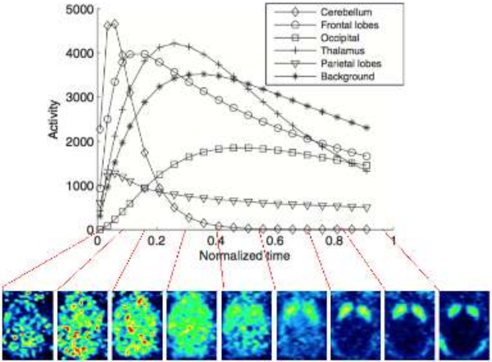

Noise in PET

- Arises from randomness during the photon-counting process
- Number of events recorded in any fixed time interval obeys the Poisson probability distribution
- Three type of coincidence events: True, Random and Scattered

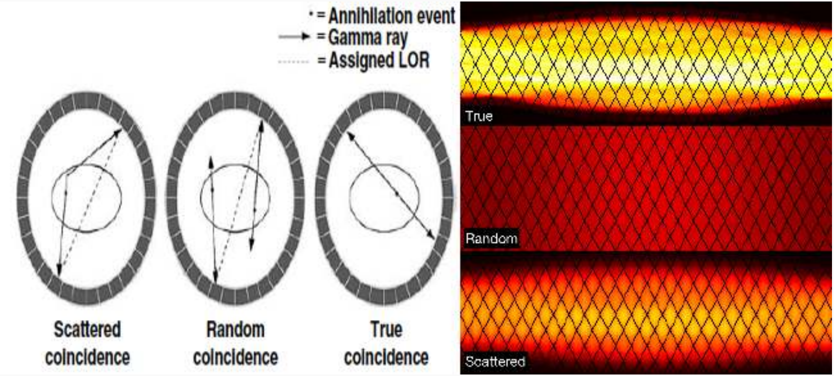

Dynamic PET

- Acquisition: “Sinogram frames” collected in a non-uniform time setting
- Late frames ⇒ Large time periods ⇒ Good counting statistics but poor temporal resolution
- Early frames ⇒ Short time periods ⇒ Noisy but preserve temporal resolution

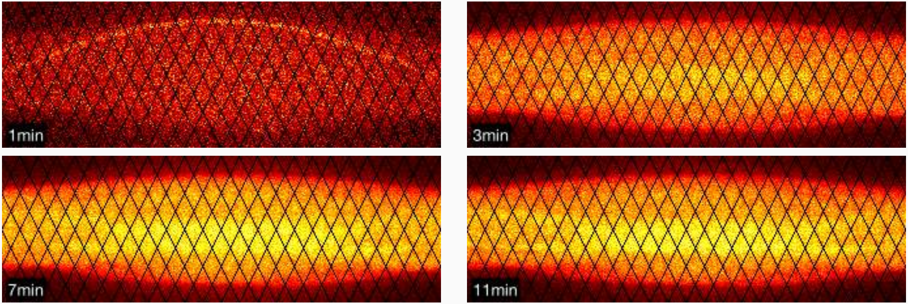

PET data for early time frames

Dynamic PET

- Acquisition: "Sinogram frames" collected in a non-uniform time setting
- Late frames ⇒ Large time periods ⇒ Good counting statistics but poor temporal resolution
- Early frames ⇒ Short time periods ⇒ Noisy but preserve temporal resolution

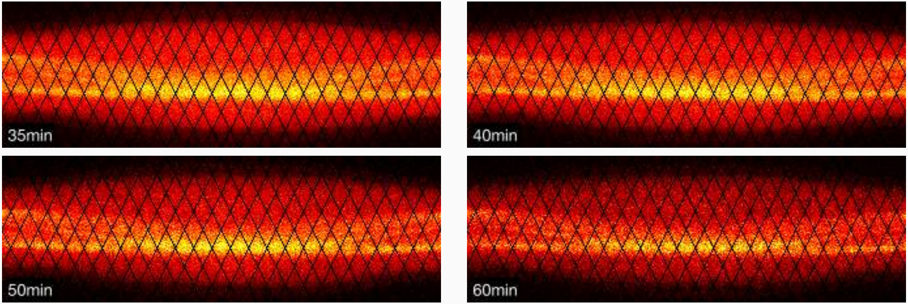

PET data for late time frames

☑ Variational framework in PET

Variational framework in PET

- Given $g = (g_{i,k}) \in \mathbb{R}^{M \times K}$, M sinogram bins, K number of frames

Variational framework in PET

- Given $g = (g_{i,k}) \in \mathbb{R}^{M \times K}$, M sinogram bins, K number of frames
- Find $u = (u_{j,k}) \in \mathbb{R}^{N \times K}$ (N spatial bins) through

Variational framework in PET

- Given $g = (g_{i,k}) \in \mathbb{R}^{M \times K}$, M sinogram bins, K number of frames
- Find $u = (u_{j,k}) \in \mathbb{R}^{N \times K}$ (N spatial bins) through

$$\min_u \mathscr{N}(u) + \mathscr{H}\left(\mathrm{R}\, u,\, g\right)$$

Variational framework in PET

- Given $g = (g_{i,k}) \in \mathbb{R}^{M \times K}$, M sinogram bins, K number of frames
- Find $u = (u_{j,k}) \in \mathbb{R}^{N \times K}$ (N spatial bins) through

$$\min_{u} \mathscr{N}(u) + \mathscr{H}\left(\mathrm{R}\, u,\, g\right)$$

R: discrete form of the Radon Transform $\mathscr{R} u_\theta(s) = \int_{y \in \theta^\perp} u(s\theta + y)\, dy$

- $$(\mathrm{R}u)_{i,k} := \sum_{j=1}^{N} R_{i,j} u_{j,k},\ 1 \leq i, k \leq M, K$$

- System matrix describes geometry of the acquisition
- Coefficients: Probability that an emitted photon from voxel j will be recorded in the ith tube of response

Variational framework in PET

- Given $g = (g_{i,k}) \in \mathbb{R}^{M \times K}$, M sinogram bins, K number of frames
- Find $u = (u_{j,k}) \in \mathbb{R}^{N \times K}$ (N spatial bins) through

$$\min_{u} \mathscr{N}(u) + \mathscr{H}\,(\mathrm{R}\,u,\, g)$$

$$g_{i,k} \sim \textbf{Poisson}\left(\gamma_k\big(\sum_{j=1}^{N} D_k \mathrm{R}_{i,j} u_{i,k} + [SC]_{i,k} + [RD]_{i,k}\big)\right)$$

- $[\mathrm{SC}]_{i,k}$, $[\mathrm{RD}]_{i,k}$: scattered and random events resp.
- D_k: Decay factor depends on the radiotracer (half-life) and frame duration.

$$A_k = A_0 \frac{1 - e^{\lambda \Delta t_k}}{e^{\lambda t_1} \lambda \Delta t_k},\ \lambda = \frac{\ln 2}{\tau_{1/2}}$$

- $\gamma_k = \Delta t_k = t_{k+1} - t_k$, $1 \leq k \leq K - 1$.

Variational framework in PET

$$\min_u \mathcal{N}(u) + \mathcal{H}\left(\mathrm{R}\, u,\, g\right)$$

- $$g_{i,k} \sim \textbf{Poisson}\Big(\gamma_k\big(\sum_{j=1}^{N} D_k \mathrm{R}_{i,j} u_{i,k} + \overbrace{[SC]_{i,k} + [RD]_{i,k}\big)}^{\eta_{i,k}}\Big)$$

$\Longrightarrow$ MAP estimation & Bayes' theorem: $\operatorname*{argmax}_u \mathbf{P}(\mathbf{u}|\mathbf{g})$

Variational framework in PET

$$\min_u \mathscr{N}(u) + \mathscr{H}\left(\mathrm{R}\, u,\, g\right)$$

$$\mathbf{P}(\boldsymbol{g}|\boldsymbol{u}) = \prod_{i,k=1}^{M,K} \frac{\gamma_k (D_k(\mathrm{R}u)_{i,k} + \eta_{i,k})^{g_{i,k}}\, e^{-\gamma_k (D_k(\mathrm{R}u)_{i,k} + \eta_{i,k})}}{g_{i,k}!}$$

$$\mathscr{P}(\boldsymbol{u}) = e^{-\mathscr{N}(\boldsymbol{u})} \quad (\text{ Prior })$$

$\Longrightarrow$ MAP estimation & Bayes' theorem: $\operatorname*{argmax}_u \mathbf{P}(\mathbf{u}|\mathbf{g})$

Variational framework in PET

$$\min_u \mathscr{N}(u) + \mathscr{H}(\mathrm{R}\, u, g)$$

$$\mathbf{P}(\boldsymbol{g}|\boldsymbol{u}) = \prod_{i,k=1}^{M,K} \frac{\gamma_k (D_k(\mathrm{R}u)_{i,k} + \eta_{i,k})^{g_{i,k}} \, e^{-\gamma_k (D_k(\mathrm{R}u)_{i,k} + \eta_{i,k})}}{g_{i,k}!}$$

$$\mathscr{P}(\boldsymbol{u}) = e^{-\mathscr{N}(\boldsymbol{u})} \quad (\text{ Prior })$$

$\Longrightarrow$ MAP estimation & Bayes' theorem: $\underset{u}{\operatorname{argmax}}$ $\mathbf{P(g|u)P(\boldsymbol{u})}$

$$\min_u \quad \mathscr{N}(u) + \sum_{i,k=1}^{M,K} \gamma_k \Big(D_k(\mathrm{R}u)_{i,k} - g_{i,k} \log \left(D_k(\mathrm{R}u)_{i,k} + \eta_{i,k} \right) \Big) + \mathbb{I}_{\{\boldsymbol{u} \geq 0\}}(\boldsymbol{u})$$

☑ TV based priors

Total Variation based priors

- Static: $\mathrm{TV}(u) = \|\nabla u\|_1 = \sum \sqrt{(\partial_x u)^2 + (\partial_y u)^2}$

Total Variation based priors

- Dynamic: $\mathrm{TV}_{\boldsymbol{\alpha}}(u) = \|\nabla_{\boldsymbol{\alpha}} u\|_1 = \sum \sqrt{(\alpha_1 \partial_x u)^2 + (\alpha_1 \partial_y u)^2 + (\alpha_2 \partial_t u)^2}$

Total Variation based priors

- Dynamic: $\mathrm{TV}_{\boldsymbol{\alpha}}(u) = \|\nabla_{\boldsymbol{\alpha}} u\|_1 = \sum \sqrt{(\alpha_1 \partial_{space} u)^2 + (\alpha_2 \partial_{time} u)^2}$

Total Variation based priors

- Dynamic: $\mathrm{TV}_{\boldsymbol{\alpha}}(u) = \|\nabla_{\boldsymbol{\alpha}} u\|_1 = \sum \sqrt{(\alpha_1 \partial_{space} u)^2 + (\alpha_2 \partial_{time} u)^2}$

- $\alpha_2 >> \alpha_1$: Strong temporal regularization
- $\alpha_2 << \alpha_1$: Weak temporal regularization
- Spatial & temporal staircasing artifacts

Total Variation based priors

- Dynamic: $\mathrm{TV}_{\boldsymbol{\alpha}}(u) = \|\nabla_{\boldsymbol{\alpha}} u\|_1 = \sum \sqrt{(\alpha_1 \partial_{space} u)^2 + (\alpha_2 \partial_{time} u)^2}$

- $\alpha_2 >> \alpha_1$: Strong temporal regularization
- $\alpha_2 << \alpha_1$: Weak temporal regularization
- Spatial & temporal staircasing artifacts

Infimal convolution approach

- Dynamic: $\mathrm{TV}_{\boldsymbol{\alpha}}(u) = \|\nabla_{\boldsymbol{\alpha}} u\|_1 = \sum \sqrt{(\alpha_1 \partial_{space} u)^2 + (\alpha_2 \partial_{time} u)^2}$

  - $\alpha_2 >> \alpha_1$: Strong temporal regularization
  - $\alpha_2 << \alpha_1$: Weak temporal regularization
  - Spatial & temporal staircasing artifacts

- Combine locally strong/weak temporal regularization via *infimal-convolution*.

$$\mathrm{ICTV}_{\boldsymbol{\beta},\boldsymbol{\kappa}}(\boldsymbol{u}) = \min_{\boldsymbol{v}} \beta_1 \, \mathrm{TV}_{\boldsymbol{\kappa}}(\boldsymbol{u} - \boldsymbol{v}) + \beta_0 \, \mathrm{TV}_{1-\boldsymbol{\kappa}}(\boldsymbol{v})$$

  - $\boldsymbol{\beta} = (\beta_1, \beta_0) > 0$ regularizing parameters
  - $\boldsymbol{\kappa} = (\kappa, 1-\kappa)$, $\kappa \in (0,1)$, $\begin{cases} \kappa \to 1 \implies \text{Spatial regularization} \\ \kappa \to 0 \implies \text{Temporal regularization} \end{cases}$
  - $\begin{array}{l} v \to 0: \ \text{Penalize } \beta_1 \, \mathrm{TV}_{\boldsymbol{\kappa}}(\boldsymbol{u}) \\ v \to u: \ \text{Penalize } \beta_0 \, \mathrm{TV}_{1-\boldsymbol{\kappa}}(\boldsymbol{u}) \end{array} \ \underbrace{\implies}_{\kappa}$ Strong or Weak temporal regularization
  - Combine both cases via $\beta_1 \, \mathrm{TV}_{\boldsymbol{\kappa}}(\boldsymbol{u} - \boldsymbol{v}) + \beta_0 \, \mathrm{TV}_{1-\boldsymbol{\kappa}}(\boldsymbol{u})$

Holler, Kunisch, 2014, SIAM IS, Benning et al, 2016

Infimal convolution approach

- $\mathrm{TV}_{\boldsymbol{\alpha}}(u) = \|\nabla_{\boldsymbol{\alpha}} u\|_1 = \sum \sqrt{(\alpha_1 \partial_{space} u)^2 + (\alpha_2 \partial_{time} u)^2}$
- $\mathrm{ICTV}_{\boldsymbol{\beta},\boldsymbol{\kappa}}(\boldsymbol{u}) = \min_{\boldsymbol{v}} \beta_1 \, \mathrm{TV}_{\boldsymbol{\kappa}}(\boldsymbol{u} - \boldsymbol{v}) + \beta_0 \, \mathrm{TV}_{1-\boldsymbol{\kappa}}(\boldsymbol{v})$

☐ Extend to high order regularization

Infimal convolution approach

- $\mathrm{TV}_{\boldsymbol{\alpha}}(u) = \|\nabla_{\boldsymbol{\alpha}} u\|_1 = \sum \sqrt{(\alpha_1 \partial_{space} u)^2 + (\alpha_2 \partial_{time} u)^2}$
- $\mathrm{ICTV}_{\boldsymbol{\beta},\boldsymbol{\kappa}}(\boldsymbol{u}) = \min_{\boldsymbol{v}} \beta_1 \, \mathrm{TV}_{\boldsymbol{\kappa}}(\boldsymbol{u} - \boldsymbol{v}) + \beta_0 \, \mathrm{TV}_{1-\boldsymbol{\kappa}}(\boldsymbol{v})$

☐ Extend to high order regularization

- $\mathrm{TGV}_{\boldsymbol{\alpha}}(\boldsymbol{u}) = \min_{\boldsymbol{v}} \|\nabla_{\boldsymbol{\alpha}} \boldsymbol{u} - \boldsymbol{v}\|_1 + \sqrt{2} \, \|\mathscr{E}_{\boldsymbol{\alpha}} \boldsymbol{v}\|_1$
  - $\mathscr{E}_{\boldsymbol{\alpha}} \boldsymbol{v} = \frac{1}{2}(\nabla_{\boldsymbol{\alpha}} \boldsymbol{v} + (\nabla_{\boldsymbol{\alpha}} \boldsymbol{v})^T)$ weighted $\boldsymbol{\alpha}$-symmetrized gradient
  - Piecewise smooth both in spatial and temporal domains

Bredies, Kunisch, Pock, SIAM IS, 2010

Infimal convolution approach

- $\mathrm{TV}_{\boldsymbol{\alpha}}(u) = \|\nabla_{\boldsymbol{\alpha}} u\|_1 = \sum \sqrt{(\alpha_1 \partial_{space} u)^2 + (\alpha_2 \partial_{time} u)^2}$
- $\mathrm{ICTV}_{\boldsymbol{\beta},\boldsymbol{\kappa}}(\boldsymbol{u}) = \min_{\boldsymbol{v}} \beta_1 \, \mathrm{TV}_{\boldsymbol{\kappa}}(\boldsymbol{u} - \boldsymbol{v}) + \beta_0 \, \mathrm{TV}_{1-\boldsymbol{\kappa}}(\boldsymbol{v})$

☐ Extend to high order regularization

- $\mathrm{TGV}_{\boldsymbol{\alpha}}(\boldsymbol{u}) = \min_{\boldsymbol{v}} \|\nabla_{\boldsymbol{\alpha}} \boldsymbol{u} - \boldsymbol{v}\|_1 + \sqrt{2} \, \|\mathscr{E}_{\boldsymbol{\alpha}} \boldsymbol{v}\|_1$
  - $\mathscr{E}_{\boldsymbol{\alpha}} \boldsymbol{v} = \frac{1}{2}(\nabla_{\boldsymbol{\alpha}} \boldsymbol{v} + (\nabla_{\boldsymbol{\alpha}} \boldsymbol{v})^T)$ weighted $\boldsymbol{\alpha}$-symmetrized gradient
  - Piecewise smooth both in spatial and temporal domains
- $$\begin{aligned} \mathrm{ICTGV}_{\boldsymbol{\beta},\boldsymbol{\kappa}}(\boldsymbol{u}) &= \min_{\boldsymbol{v}} \beta_1 \, \mathrm{TGV}_{\boldsymbol{\kappa}}(\boldsymbol{u} - \boldsymbol{v}) + \beta_0 \, \mathrm{TGV}_{1-\boldsymbol{\kappa}}(\boldsymbol{v}) \\ &= \min_{\boldsymbol{v}, \boldsymbol{w_1}, \boldsymbol{w_2}} \beta_1 \, \|\nabla_{\boldsymbol{\kappa}}(\boldsymbol{u} - \boldsymbol{v}) - \boldsymbol{w_1}\|_1 + \beta_1 \sqrt{2} \, \|\mathscr{E}_{\boldsymbol{\kappa}} \boldsymbol{w_1}\|_1 \\ &\quad + \beta_0 \, \|\nabla_{\mathbf{1}-\boldsymbol{\kappa}} \boldsymbol{v} - \boldsymbol{w_2}\|_1 + \beta_0 \sqrt{2} \, \|\mathscr{E}_{\mathbf{1}-\boldsymbol{\kappa}} \boldsymbol{w_2}\|_1 \end{aligned}$$
  - Combine smoothness of TGV and inf-conv approach

Schloegl et al, Magn Reson Med, 2017

☑ Numerical implementation

Numerical implementation

- X,Y with $\dim X = n$, $\dim Y = m$
- $\mathscr{K} \in \mathscr{L}(X, Y)$, $\|\mathscr{K}\| = \max\{\|\mathscr{K}x\|_Y : \|x\|_X \leq 1\}$
- $\mathscr{G}, \mathscr{F} : X, Y \to \overline{\mathbb{R}}$ proper, convex, lsc
- Resolvent operators e.g., $x = (I + \tau\partial\mathscr{G})^{-1}(\hat{x}) \Longrightarrow$ closed form solutions

Numerical implementation

- X,Y with $\dim X = n$, $\dim Y = m$
- $\mathscr{K} \in \mathscr{L}(X, Y)$, $\|\mathscr{K}\| = \max\{\|\mathscr{K}x\|_Y : \|x\|_X \leq 1\}$
- $\mathscr{G}, \mathscr{F} : X, Y \to \overline{\mathbb{R}}$ proper, convex, lsc
- Resolvent operators e.g., $x = (I + \tau\partial\mathscr{G})^{-1}(\hat{x}) \implies$ closed form solutions

$$\min_u \quad \mathscr{N}(u) + \sum_{i,k=1}^{M,K} \gamma_k \Big(D_k(\mathrm{R}u)_{i,k} - g_{i,k} \log\left(D_k(\mathrm{R}u)_{i,k} + \eta_{i,k}\right)\Big) + \mathbb{I}_{\{\boldsymbol{u} \geq 0\}}(\boldsymbol{u})$$

$$\mathscr{N}(\boldsymbol{u}) = \{\mathrm{TV}_{\boldsymbol{\alpha}}(\boldsymbol{u}), \mathrm{ICTV}_{\boldsymbol{\beta},\boldsymbol{\kappa}}(\boldsymbol{u}), \mathrm{TGV}_{\boldsymbol{\alpha}}(\boldsymbol{u}), \mathrm{ICTGV}_{\boldsymbol{\beta},\boldsymbol{\kappa}}(\boldsymbol{u})\}$$

Numerical implementation

- X,Y with $\dim X = n$, $\dim Y = m$
- $\mathscr{K} \in \mathscr{L}(X, Y)$, $\|\mathscr{K}\| = \max\{\|\mathscr{K}x\|_Y : \|x\|_X \leq 1\}$
- $\mathscr{G}, \mathscr{F} : X, Y \to \overline{\mathbb{R}}$ proper, convex, lsc

$$\min_u \quad \mathscr{N}(u) + \sum_{i,k=1}^{M,K} \gamma_k \Big(D_k(\mathrm{R}u)_{i,k} - g_{i,k} \log\left(D_k(\mathrm{R}u)_{i,k} + \eta_{i,k}\right) \Big) + \mathbb{I}_{\{\boldsymbol{u} \geq 0\}}(\boldsymbol{u})$$

Numerical implementation

- X,Y with $\dim X = n$, $\dim Y = m$
- $\mathscr{K} \in \mathscr{L}(X, Y)$, $\|\mathscr{K}\| = \max\{\|\mathscr{K}x\|_Y : \|x\|_X \leq 1\}$
- $\mathscr{G}, \mathscr{F} : X, Y \to \overline{\mathbb{R}}$ proper, convex, lsc

$$\min_x \quad \mathscr{F}(\mathscr{K}x) + \mathscr{G}(x)$$

Numerical implementation

- X,Y with $\dim X = n$, $\dim Y = m$
- $\mathscr{K} \in \mathscr{L}(X, Y)$, $\|\mathscr{K}\| = \max\{\|\mathscr{K}x\|_Y : \|x\|_X \leq 1\}$
- $\mathscr{G}, \mathscr{F} : X, Y \to \overline{\mathbb{R}}$ proper, convex, lsc

$$\min_x \quad \mathscr{F}(\mathscr{K}x) + \mathscr{G}(x) \quad \text{(Primal)}$$

Numerical implementation

- X,Y with $\dim X = n$, $\dim Y = m$
- $\mathscr{K} \in \mathscr{L}(X, Y)$, $\|\mathscr{K}\| = \max\{\|\mathscr{K}x\|_Y : \|x\|_X \leq 1\}$
- $\mathscr{G}, \mathscr{F} : X, Y \to \overline{\mathbb{R}}$ proper, convex, lsc

$$\min_x \quad \mathscr{F}(\mathscr{K}x) + \mathscr{G}(x) \quad \text{(Primal)}$$

$$\min_{x \in X} \max_{y \in Y} \langle \mathscr{K}x, y \rangle_Y + \mathscr{G}(x) - \mathscr{F}^*(y) \text{ (Primal - Dual)}$$

Numerical implementation

- X,Y with $\dim X = n$, $\dim Y = m$
- $\mathscr{K} \in \mathscr{L}(X, Y)$, $\|\mathscr{K}\| = \max\{\|\mathscr{K}x\|_Y : \|x\|_X \leq 1\}$
- $\mathscr{G}, \mathscr{F} : X, Y \to \overline{\mathbb{R}}$ proper, convex, lsc

$$\min_{x} \quad \mathscr{F}(\mathscr{K}x) + \mathscr{G}(x) \quad \text{(Primal)}$$

$$\min_{x \in X} \max_{y \in Y} \langle \mathscr{K}x, y\rangle_Y + \mathscr{G}(x) - \mathscr{F}^*(y) \text{ (Primal - Dual)}$$

$$\max_{y \in Y} -\mathscr{G}^*(-\mathscr{K}^T y) - \mathscr{F}^*(y) \text{ (Dual Problem)}$$

Numerical implementation

- X,Y with $\dim X = n$, $\dim Y = m$
- $\mathscr{K} \in \mathscr{L}(X, Y)$, $\|\mathscr{K}\| = \max\{\|\mathscr{K}x\|_Y : \|x\|_X \leq 1\}$
- $\mathscr{G}, \mathscr{F} : X, Y \to \overline{\mathbb{R}}$ proper, convex, lsc

$$\min_{x} \quad \mathscr{F}(\mathscr{K}x) + \mathscr{G}(x) \quad \text{(Primal)}$$

$$\min_{x\in X} \max_{y\in Y} \langle \mathscr{K}x, y\rangle_Y + \mathscr{G}(x) - \mathscr{F}^*(y) \text{ (Primal - Dual)}$$

$$\max_{y\in Y} -\mathscr{G}^*(-\mathscr{K}^T y) - \mathscr{F}^*(y) \text{ (Dual Problem)}$$

- Compute *primal-dual* gap to measure optimality

$$PD_{gap} = \mathscr{F}(\mathscr{K}x) + \mathscr{G}(x) + \mathscr{F}^*(-y) + \mathscr{G}^*(-\mathscr{K}^T y)$$

$\implies$ Set $\mathscr{K}, \mathscr{G}$ and $\mathscr{F}$ for each

$$\mathscr{N}(\boldsymbol{u}) = \{\mathrm{TV}_{\boldsymbol{\alpha}}(\boldsymbol{u}), \mathrm{ICTV}_{\boldsymbol{\beta},\boldsymbol{\kappa}}(\boldsymbol{u}), \mathrm{TGV}_{\boldsymbol{\alpha}}(\boldsymbol{u}), \mathrm{ICTGV}_{\boldsymbol{\beta},\boldsymbol{\kappa}}(\boldsymbol{u})\}$$

Numerical implementation

Primal-Dual gradient method

$$\min_{x\in X}\max_{y\in Y} \langle \mathscr{K} x, y\rangle_Y + \mathscr{G}(x) - \mathscr{F}^*(y)$$

- Chambolle-Pock algorithm
  - $\tau, \sigma \in \mathbb{R}_{++}$, $\theta \in (0,1)$, $(x_0, y_0) \in X \times Y$

Update: x_ω, y_ω

$$\begin{cases} x_{\omega+1} = (I + \tau\partial\mathscr{G})^{-1}(x_\omega - \tau\mathscr{K}^T y_\omega) \\ \overline{x}_{\omega+1} = x_{\omega+1} + \theta(x_{\omega+1} - x_\omega) \\ y_{\omega+1} = (I + \sigma\partial\mathscr{F}^*)^{-1}\left(y_\omega + \sigma\mathscr{K}(\overline{x}_{\omega+1})\right) \end{cases}$$

  - Convergence: $\theta = 1$ and $\tau\sigma\|\mathscr{K}\| < 1$

Chambolle, Pock, JMIV, 2010

Numerical implementation

Primal-Dual gradient method

$$\min_{x\in X}\max_{y\in Y}\langle \mathscr{K}x, y\rangle_Y + \mathscr{G}(x) - \mathscr{F}^*(y)$$

- Chambolle-Pock algorithm (Diagonal Preconditioning)

  - T, Σ, SPD, $\theta \in [0,1]$ and $(x_0, y_0) \in X \times Y$

Update: x_ω, y_ω

$$\begin{cases} x_{\omega+1} = (I + T\partial\mathscr{G})^{-1}(x_\omega - T\mathscr{K}^T y_\omega) \\ \overline{x}_{\omega+1} = x_{\omega+1} + \theta(x_{\omega+1} - x_\omega) \\ y_{\omega+1} = (I + \Sigma\partial\mathscr{F}^*)^{-1}\left(y_\omega + \Sigma\mathscr{K}(\overline{x}_{\omega+1})\right) \end{cases}$$

  - Convergence: $\theta = 1$ and $\left\|\Sigma^{1/2}\mathscr{K}T^{1/2}\right\| < 1$,

$$T = \mathrm{diag}(\boldsymbol{\tau}),\ \Sigma = \mathrm{diag}(\boldsymbol{\sigma})$$

$$\tau_j = \frac{1}{\sum_{i=1}^m |\mathscr{K}_{i,j}|^{2-\alpha}}, \quad \sigma_i = \frac{1}{\sum_{j=1}^n |\mathscr{K}_{i,j}|^{\alpha}},\ \alpha \in [0,2].$$

Chambolle, Pock, ICCV, 2011, Goldstein et al, 2013

Numerical implementation

Example: $\mathrm{ICTV}_{\boldsymbol{\beta},\boldsymbol{\kappa}}(\boldsymbol{u})$ case

$$\min_{\boldsymbol{u},\boldsymbol{v}} \quad \beta_1 \|\nabla_{\boldsymbol{\kappa}}(\boldsymbol{u}-\boldsymbol{v})\|_1 + \beta_0 \|\nabla_{\mathbf{1}-\boldsymbol{\kappa}}\boldsymbol{v}\|_1 + \sum \boldsymbol{\gamma}\Big(D(\mathrm{R}\boldsymbol{u}) - \boldsymbol{g}\log\big(D(\mathrm{R}\boldsymbol{u})+\boldsymbol{\eta}\big)\Big) + \mathbb{I}_{\{\boldsymbol{u}\geq 0\}}(\boldsymbol{u})$$

Numerical implementation

Example: $\mathrm{ICTV}_{\boldsymbol{\beta},\boldsymbol{\kappa}}(\boldsymbol{u})$ case

$$\min_{\boldsymbol{u},\boldsymbol{v}} \max_{\boldsymbol{\phi_1},\boldsymbol{\phi_2}} \langle \nabla_{\boldsymbol{\kappa}}(\boldsymbol{u}-\boldsymbol{v}), \boldsymbol{\phi_1}\rangle - \mathbb{I}_{\{\|\cdot\|_\infty \leq \beta_1\}}\left(\frac{\boldsymbol{\phi_1}}{\gamma}\right) + \langle \nabla_{\boldsymbol{1}-\boldsymbol{\kappa}}, \boldsymbol{\phi_2}\rangle - \mathbb{I}_{\{\|\cdot\|_\infty \leq \beta_0\}}\left(\frac{\boldsymbol{\phi_2}}{\gamma}\right)$$
$$+ \left\langle \gamma(D\mathrm{R}\boldsymbol{u} - \boldsymbol{g}\log(D\mathrm{R}\boldsymbol{u}+\boldsymbol{\eta})), 1_{\hat{U}}\right\rangle + \mathbb{I}_{\{\boldsymbol{u}\geq 0\}}(\boldsymbol{u})$$

Numerical implementation

Example: $\mathrm{ICTV}_{\boldsymbol{\beta},\boldsymbol{\kappa}}(\boldsymbol{u})$ case

$$\min_{\boldsymbol{u},\boldsymbol{v}} \max_{\phi_1,\phi_2,\phi_3} \langle \nabla_{\boldsymbol{\kappa}}(\boldsymbol{u}-\boldsymbol{v}), \boldsymbol{\phi_1}\rangle - \mathbb{I}_{\{\|\cdot\|_\infty \le \beta_1\}}\left(\frac{\boldsymbol{\phi_1}}{\gamma}\right) + \langle \nabla_{\mathbf{1}-\boldsymbol{\kappa}}, \boldsymbol{\phi_2}\rangle - \mathbb{I}_{\{\|\cdot\|_\infty \le \beta_0\}}\left(\frac{\boldsymbol{\phi_2}}{\gamma}\right)$$
$$+ \langle \mathrm{R}u, \boldsymbol{\phi_3}\rangle - \mathscr{H}^*(\boldsymbol{g}, \boldsymbol{\phi_3}) + \mathbb{I}_{\{\boldsymbol{u}\ge 0\}}(\boldsymbol{u})$$

Numerical implementation

Example: $\mathrm{ICTV}_{\boldsymbol{\beta},\boldsymbol{\kappa}}(\boldsymbol{u})$ case

$$\min_{\boldsymbol{u},\boldsymbol{v}} \max_{\phi_1,\phi_2,\phi_3} \langle \nabla_{\boldsymbol{\kappa}}(\boldsymbol{u}-\boldsymbol{v}), \boldsymbol{\phi_1}\rangle - \mathbb{I}_{\{\|\cdot\|_\infty \le \beta_1\}}(\frac{\boldsymbol{\phi_1}}{\boldsymbol{\gamma}}) + \langle \nabla_{\mathbf{1}-\boldsymbol{\kappa}}, \boldsymbol{\phi_2}\rangle - \mathbb{I}_{\{\|\cdot\|_\infty \le \beta_0\}}(\frac{\boldsymbol{\phi_2}}{\boldsymbol{\gamma}}) + \langle \mathrm{R}u, \boldsymbol{\phi_3}\rangle - \mathscr{H}^*(\boldsymbol{g}, \boldsymbol{\phi_3}) + \mathbb{I}_{\{\boldsymbol{u}\ge 0\}}(\boldsymbol{u})$$

$$\min_{x\in X} \max_{y\in Y} \langle \mathscr{K} x, y\rangle_Y + \mathscr{G}(x) - \mathscr{F}^*(y)$$

$$\begin{cases} \mathscr{F}^*(y) = \mathscr{F}^*(\boldsymbol{\phi_1}, \boldsymbol{\phi_2}, \boldsymbol{\phi_3}) = \mathbb{I}_{\{\|\cdot\|_\infty \le \beta_1\}}(\frac{\boldsymbol{\phi_1}}{\boldsymbol{\gamma}}) + \mathbb{I}_{\{\|\cdot\|_\infty \le \beta_0\}}(\frac{\boldsymbol{\phi_2}}{\boldsymbol{\gamma}}) + \mathscr{H}^*(\boldsymbol{g}, \boldsymbol{\phi_3}) \\ \mathscr{G}(x) = \mathscr{G}(\boldsymbol{u}, \boldsymbol{v}) = \mathbb{I}_{\{\boldsymbol{u}\ge 0\}}(\boldsymbol{u}), \\ \mathscr{H}^*(\boldsymbol{g}, \boldsymbol{\phi_3}) = \sum \boldsymbol{\gamma}\boldsymbol{g}\left(\log\left(\frac{\boldsymbol{\gamma}\boldsymbol{D}\boldsymbol{g}}{\boldsymbol{\gamma}\boldsymbol{D}-\boldsymbol{\phi_3}}\right) - 1\right) - \boldsymbol{\eta}(\frac{\boldsymbol{\phi_3}}{\boldsymbol{D}} - \gamma) + \mathbb{I}_{\{\boldsymbol{\phi_3} \ge \boldsymbol{\gamma}\boldsymbol{D} - \boldsymbol{g}\frac{\boldsymbol{\gamma}\boldsymbol{D}}{\boldsymbol{\eta}}\}}(\boldsymbol{\phi_3}) \\ \mathscr{K} = \begin{bmatrix} \nabla_{\boldsymbol{\kappa}} & -\nabla_{\boldsymbol{\kappa}} \\ 0 & \nabla_{\mathbf{1}-\boldsymbol{\kappa}} \\ \mathrm{R} & 0 \end{bmatrix}, \mathscr{K}^T = \begin{bmatrix} -\mathrm{div}_{1,\boldsymbol{\kappa}} & 0 & \mathrm{R}^* \\ \mathrm{div}_{1,\boldsymbol{\kappa}} & \mathrm{div}_{1,\mathbf{1}-\boldsymbol{\kappa}} & 0 \end{bmatrix} \end{cases}$$

☑ Dynamic PET simulation

Dynamic PET simulation

- Analytic simulations using Realistic count rates
    - Extract parameters from real patient scans

Dynamic PET simulation

- Analytic simulations using Realistic count rates
- High resolution phantom with labeled regions

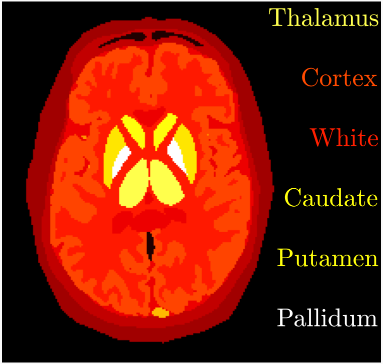

Dynamic PET simulation

- Analytic simulations using Realistic count rates
- High resolution phantom with labeled regions
- Projecting input emission distribution
  - Apply Poisson noise based on total number of prompts $\Longrightarrow$ Direct problem

Dynamic PET simulation

- Analytic simulations using Realistic count rates
- High resolution phantom with labeled regions
- Projecting input emission distribution
- Use TACs from real acquititions
  - Healthy patients injected with 11C-PE2i, 18F-FDG
  - ROIs delineated on T1-weighted MRI
  - Noisy real TACs $\Longrightarrow$ Apply local Gaussian smoothing for each frame

Dynamic PET simulation

- Analytic simulations using Realistic count rates
- High resolution phantom with labeled regions
- Projecting input emission distribution
- Use TACs from real acquisitions

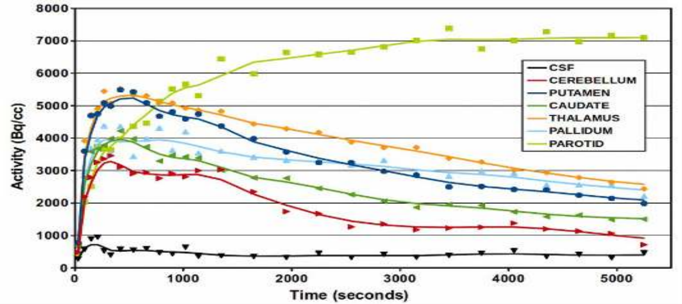

TACs from healthy patient: Dots Real TACs, Solid Smoothed versions
Act as input to the simulations

Stute et al, NSS/MIC, 2015

Dynamic PET simulation

- Analytic simulations using Realistic count rates
- High resolution phantom with labeled regions
- Projecting input emission distribution
- Use TACs from real acquisitions
- Project emission & attenuation maps
    - Real crystal coordinates $\Longrightarrow$ Siemens Biograph Hirez 4 rings
    - Frame duration & decay factor depending on the radionuclide
    - Scatter and random fractions extracted for real acquititions

Dynamic PET simulation

- Analytic simulations using Realistic count rates
- High resolution phantom with labeled regions
- Projecting input emission distribution
- Use TACs from real acquisitions
- Project emission & attenuation maps
  - Real crystal coordinates $\Longrightarrow$ Siemens Biograph Hirez 4 rings
  - Frame duration & decay factor depending on the radionuclide
  - Scatter and random fractions extracted for real acquititions

	Isotope	Prompt Counts	$\tau_{1/2}$	Duration (Frames $\times$ sec)
PE2i	^{11}C	31 000 000	1223 sec	$5 \times 60, 5 \times 120, 2 \times 150, 8 \times 300$
FDG	^{18}F	47 767 000	6586.2 sec	$5 \times 60, 5 \times 120, 2 \times 150, 8 \times 300$

Dynamic PET simulation

- Analytic simulations using Realistic count rates
- High resolution phantom with labeled regions
- Projecting input emission distribution
- Use TACs from real acquisitions
- Project emission & attenuation maps

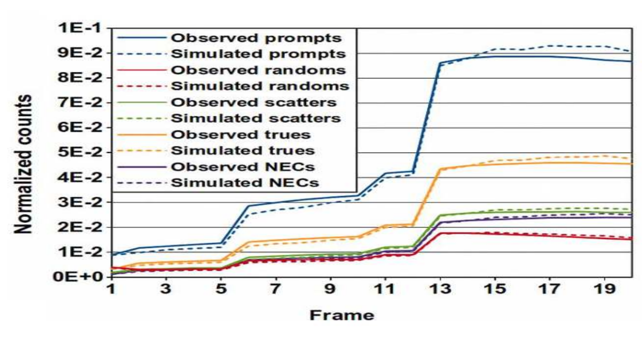

Observed and simulated count rates for ^{18}F-FDG per time-frame

☑ Results

Results: PET radiotracers

- Spatial reconstructions $\mathrm{TV}_{\alpha_1,0}$, $\mathrm{TGV}_{\alpha_1,0}$
- MLEM and post-filtered MLEM reconstructions
- Spatiotemporal reconstructions $\mathrm{TV}_{\boldsymbol{\alpha}}(\boldsymbol{u})$, $\mathrm{ICTV}_{\boldsymbol{\beta},\boldsymbol{\kappa}}(\boldsymbol{u})$, $\mathrm{TGV}_{\boldsymbol{\alpha}}(\boldsymbol{u})$, $\mathrm{ICTGV}_{\boldsymbol{\beta},\boldsymbol{\kappa}}(\boldsymbol{u})$
- Parameters are optimized in terms of average SSIM over time-frames.
- Zubal phantom 128x128x64 of 20 frames (1hour) (2.2x2.2x2.8mm^3)
- Extract dynamic data 2D+time $\Rightarrow$ 128x128x20
- PE2i: Dopamine related disorders, Parkinson, depression, alcoholism
  $\Longrightarrow$ High striatal uptake
- FDG: Glucose metabolism, cancer diagnosis and monitoring, Alzheimer
  $\Longrightarrow$ High gray matter uptake

Results: Spatial, PE2i

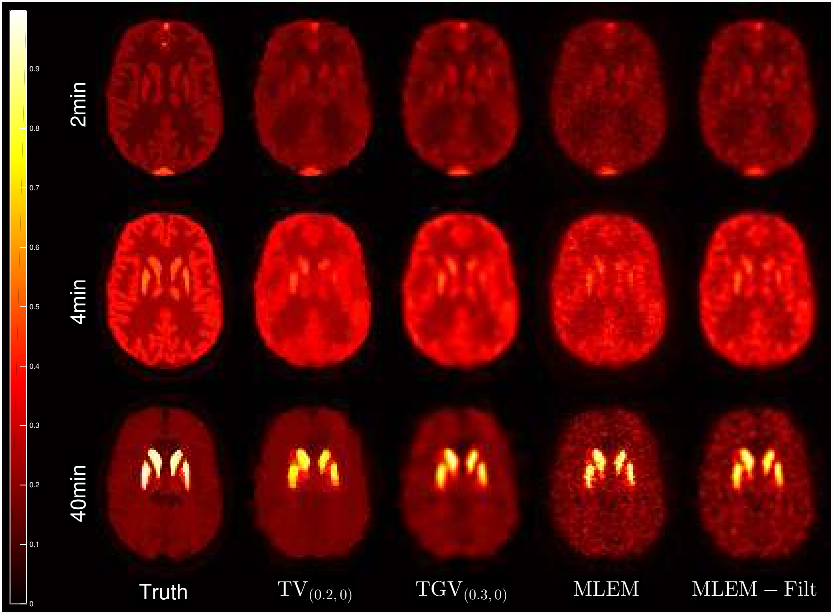

Results: Spatiotemporal, PE2i

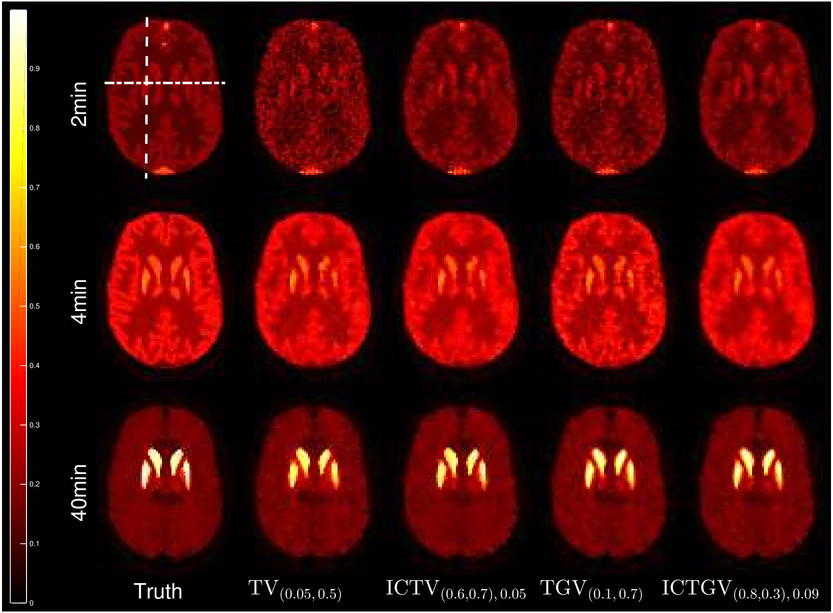

Results: Spatiotemporal, PE2i

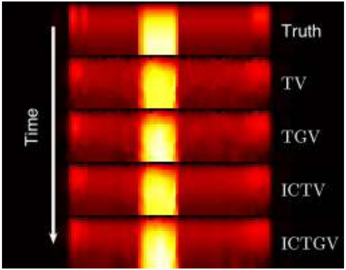

Time line

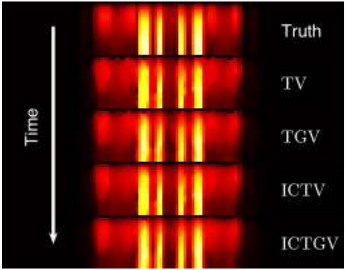

Time line

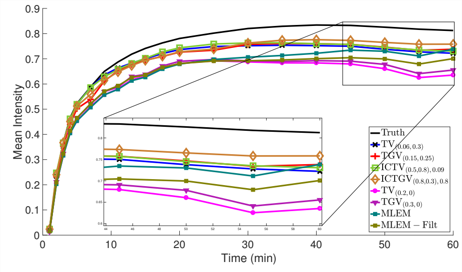

Striatum activity

Results: Spatiotemporal, PE2i

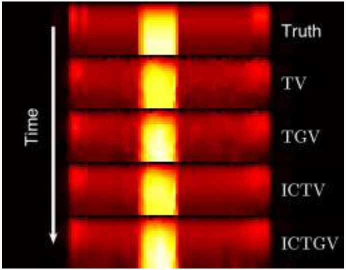

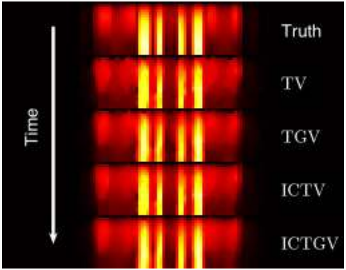

	SSIM	MSE (10^{-3})	BIAS
$TV_{(0.06,0.3)}$	0.9396	1.3181	0.3422
$TGV_{(0.15,0.25)}$	0.9417	1.3281	0.3580
$ICTV_{(0.5,0.8),0.09}$	**0.9484**	**1.1251**	**0.3105**
$ICTGV_{(0.8,0.3),0.8}$	0.9466	1.1266	0.3201
$TV_{(0.2,0)}$	0.9155	2.4955	0.3926
$TGV_{(0.3,0)}$	0.9099	2.5429	0.4485
MLEM	0.7899	3.4633	0.5402
MLEM-Filt	0.8586	2.6265	0.4767

Results: Spatiotemporal, PE2i

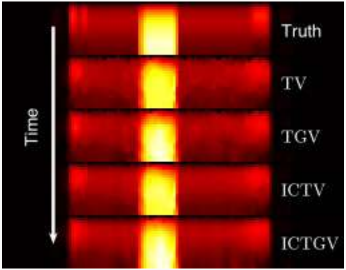

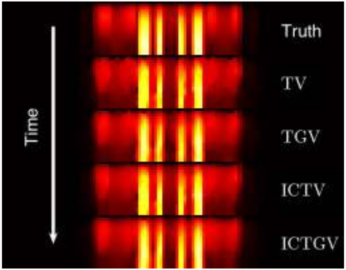

Results: Spatial, FDG

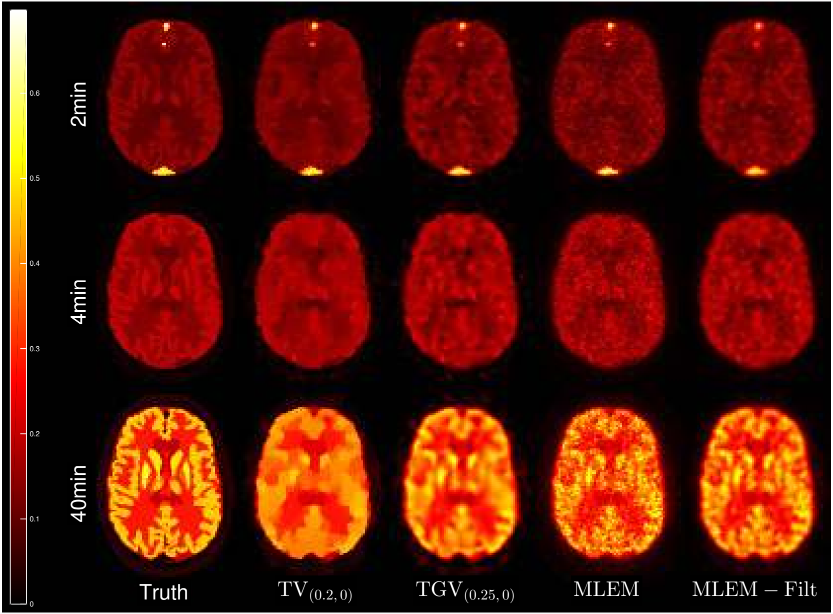

Results: Spatiotemporal, FDG

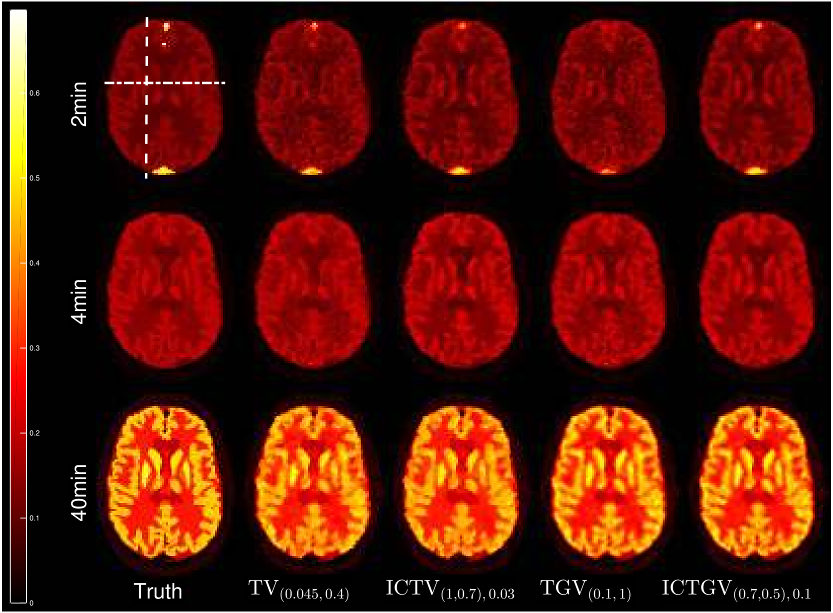

Results: Spatiotemporal, FDG

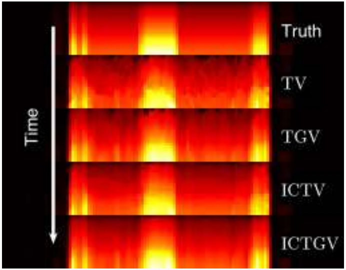

Time line

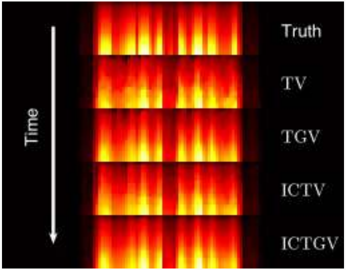

Time line

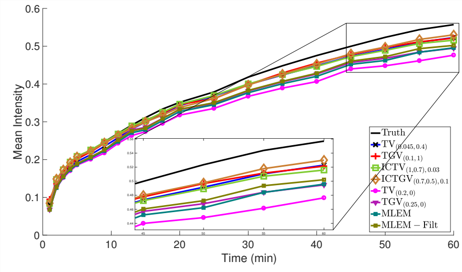

Striatum activity

Results: Spatiotemporal, FDG

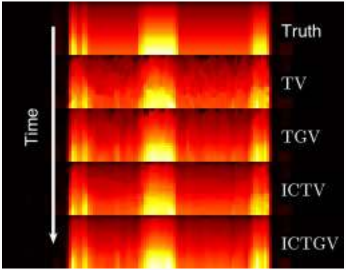

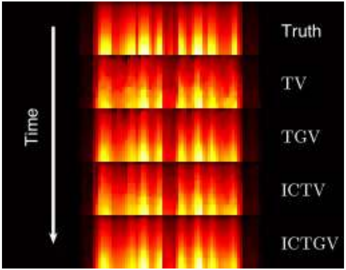

	SSIM	MSE (10^{-3})	BIAS
$TV_{(0.045,0.4)}$	0.9534	0.8787	0.2332
$TGV_{(0.1,1)}$	0.9604	0.8132	0.2243
$ICTV_{(1,0.7),0.03}$	0.9648	0.7593	0.2165
$ICTGV_{(0.7,0.5),0.1}$	**0.9686**	**0.6348**	**0.2062**
$TV_{(0.2,0)}$	0.9138	1.6369	0.3380
$TGV_{(0.25,0)}$	0.9185	1.4988	0.3656
MLEM	0.8379	2.1210	0.4347
MLEM-Filt	0.9000	1.6007	0.4084

Results: Spatiotemporal, FDG

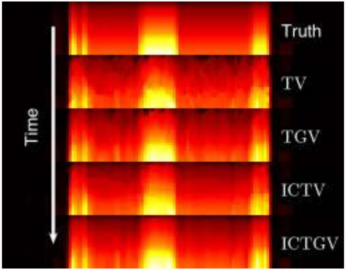

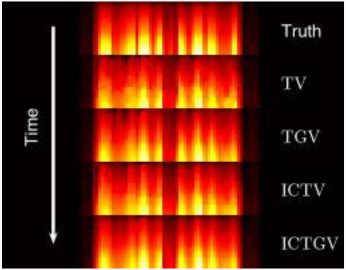

Conclusion

- Dynamic PET reconstruction using variational methods
- TV based priors and inf-conv variants
- ICTV and ICTGV behave better for different dynamics
- Fast implementation using preconditioning PDHG methods
- Simulated dynamic data with realistic PET count rates

▶ *An Anisotropic Inf-Convolution BV Type Model for Dynamic Reconstruction*
M. Bergounioux, E.P, SIAM Journal on Imaging Sciences 11 (1), 129-163

▶ *Infimal convolution spatiotemporal PET reconstruction using total variation based priors*, M.Bergounioux, E.P, S. Stute, C. Tauber,
(hal.archives-ouvertes.fr/hal-01694064)

Thank you for your attention!!!